Substrate fate in activated macrophages: A comparison between innate, classic and alternative activation

Juan-Carlos Rodríguez-Prados[*,‖], Paqui G. Través[†,‖], Jimena Cuenca[†], Daniel Rico[‡], Marta Cascante[*,¶] and Lisardo Boscá[†,§,¶]

[*]Department of Biochemistry and Molecular Biology, Institute of Biomedicine of the University of Barcelona (IBUB). Avinguda Diagonal 645, 08028 Barcelona
[†]Instituto de Investigaciones Biomédicas 'Alberto Sols' (CSIC-UAM), Arturo Duperier 4, 28029 Madrid.
[‡]Centro Nacional de Investigaciones Oncológicas (CNIO), Melchor Fernández de Almagro, 3, 28029 Madrid.
[§]Centro de Investigación Biomédica en Red de Enfermedades Hepáticas y Digestivas (Ciberehd).

[¶] *Corresponding authors*
JCRP and PGT contributed equally to this work

Address for correspondence:
Dr Lisardo Boscá
Instituto de Investigaciones Biomédicas 'Alberto Sols' (CSIC-UAM)
Arturo Duperier 4
28029 Madrid, Spain
Fax: 34915854401; e-mail: lbosca@iib.uam.es
or
Dr Marta Cascante
Department of Biochemistry and Molecular Biology
Faculty of Biology (edifici Nou) Planta -2
Avinguda Diagonal 645
08028 Barcelona, Spain
Fax: 34934021559; e-mail: marta.cascante@ub.edu

Running title: *Metabolic fluxes in macrophage activation*

Grant support: JCRP is supported by a BRD fellowship from the University of Barcelona. This work was supported by the European Commission (FP7) Etherpath KBBE-grant agreement nº 222639, the Spanish Government and the Union FEDER funds (SAF2008-00164) and ISCIII-RTICC (RD6/0020/0046) and grants SAF2005-01627 and BFU2008-02161 from Ministerio de Ciencia e Innovación of the Spanish Government, 2005SGR00204 from the Generalitat de Catalunya, S-BIO-0283/2006 from Comunidad de Madrid and FIS-RECAVA RD06/0014/0025. RECAVA and Ciberehd are funded by the Instituto de Salud Carlos III.

Abstract

Macrophages play a relevant role in innate and adaptive immunity depending on the balance of the stimuli received. From an analytical and functional point of view, macrophage stimulation can be segregated into three main topics: innate, classic and alternative pathways. These differential activations result in the expression of specific sets of genes involved in the release of pro- or anti-inflammatory stimuli. In previous works, it has been described an enhancement of metabolic pathways in the activation process and, in the present work, we have analyzed whether these metabolic pattern changes depend on the signaling pathway activated. A [1,2-$^{13}C_2$]-glucose tracer-based metabolomics approach has been used to characterize the metabolic flux distributions in peritoneal macrophages and in the RAW 264.7 cell line stimulated through the classic, innate and alternative pathways. Using this methodology combined with mass isotopomer distribution analysis (MIDA) of the new formed metabolites, the data show that activated macrophages are essentially glycolytic cells and a clear cut-off between the classic/innate activation and the alternative pathway exists. Interestingly, macrophage activation through LPS/IFN-γ, or TLR-2, -3, -4 and -9 results in similar flux distribution patterns regardless the pathway activated, despite the use of distinct signaling pathways. However, stimulation through the alternative pathway has minor metabolic effects. The molecular basis of the differences between these two types of behavior appear to involve a switch in the expression of 6-phosphofructo-2-kinase/fructose-2,6-bisphosphatase resulting in a more active enzyme and an increase in the levels of fructose-2,6-bisphosphate.

Introduction

The innate immune system acts as the first line of defense and functions by recognizing highly conserved sets of molecular patterns (PAMPs) through a limited set of germ line encoded receptors called pattern-recognition receptors (PRRs). Toll-like receptors (TLRs), a class of PRRs, have the ability to recognize pathogens or pathogen-derived products and initiate signaling events leading to activation of innate host defense (1, 2). Macrophages play an essential role in the immune response and normal tissue development by producing proinflammatory mediators and through clearance of pathogens and apoptotic cells by phagocytosis. Macrophages participate actively in the inflammatory response by releasing cytokines, chemokines and factors that recruit additional cells to sites of infection or tissue injury or alteration (3, 4). It has been described that macrophages could undergo different activation processes depending on the stimuli received (5, 6): The classic activation, that can be induced by in vitro culture of macrophages with IFN-γ and LPS (inducing TNF-α production), is associated with high microbicidal activity, pro-inflammatory cytokine and reactive oxygen species (ROS) production and cellular immunity; the innate activation, that is mediated in culture by ligation of receptors such as TLRs, most of which are expressed by cells of the monocyte–macrophage lineage, and is associated with microbicidal activity and pro-inflammatory cytokine production; the alternative activation, that can be mimicked in vitro after culture with IL-4, IL-13, glucocorticoids, immune complexes or IL-10 and is associated with tissue repair, tumor progression and humoral immunity. Some authors also distinguish macrophage deactivation, which is induced by cytokines such as IL-10 or TGF-β, or by ligation of inhibitory receptors such as CD200 receptor or CD172a, and is related to anti-inflammatory cytokine production and reduced MHC class II expression.

Under normal conditions, macrophages are recruited, invade and phagocyte at sites of infection. However, deregulated clearance of activated macrophages may lead to septic shock or chronic inflammatory diseases, including atherosclerosis and rheumatoid arthritis (4). Interestingly, in addition to playing a crucial role in immunity, some of the mammalian TLRs have been described to regulate bodily energy metabolism, mostly through acting on adipose tissue. This has recently opened new avenues of research on the role of TLRs in pathologies related to metabolism, such as obesity, insulin resistance, metabolic syndrome or atherosclerosis (7). The accumulation of fatty acids, above all cholesterol in LDL form, is the main reason why lipid metabolism has been studied in macrophages in the atherosclerosis framework. Recent works have built a fatty acid bridge between diet and immune system due to the induction of TLR expression by some fatty acids (8). However, few are know on central metabolism patterns in macrophages since the work of Newsholme and collaborators in the 90's (9-11). Here we will apply a system biology approach to shed some light in the crosstalk between signal transduction and central metabolism in macrophages. We studied whether the distinct stimulation pathways required different energy demands or have different metabolic

patterns. To achieve these goals, tracer-based metabolomics experiments have been used and combined with analysis of the expression of markers of activation. Following the normal activation process of the macrophages, cells were fed with [1,2-$^{13}C_2$]-glucose, a non radioactive isotope of glucose which behaves as the "non-label" glucose but will incorporate [^{13}C] carbons to the metabolite end products (i.e. lactate, glutamate) and in the ribose of RNA. This tracer has been broadly used before (12). Our data show that activated macrophages are essentially glycolytic cells and a clear cut-off between the classic/innate activation and the alternative pathway exists. Interestingly, activation through TLR-2, -3, -4 and -9 results in similar patterns of metabolic activation, despite the use of at least in part distinct signaling pathways and expression of different sets of genes.

Materials and Methods

Chemicals. Reagents were from Sigma (St Louis, MO), Roche (Basel, CH), Invitrogen (Carlsbad, CA), Invivogen (San Diego, CA), PeproTech (Rocky Hill, NJ) or Merck (Darmstadt, FRG). Commercial antibodies were from Santa Cruz Biotech (Santa Cruz, CA), Cell signaling (Danvers, MA), Abcam (Cambridge, UK), R&D Systems (Minneapolis, MN), Sigma or PeproTech. Serum and media were from BioWhittaker (Walkersville, MD). [1,2-$^{13}C_2$]-glucose (> 99 % enriched) was purchased from Isotec (Miamisburg, OH).

Treatment of animals and preparation of peritoneal macrophages. Animals were used aged 8 to 12-weeks as follows: Four days prior to the assay, mice were i.p. injected 2.5 ml of 3% (weight/vol) of thioglycollate broth (13). Elicited peritoneal macrophages were prepared from light-ether anesthetized mice (4-6 animals per condition), killed by cervical dislocation and injected i.p. 10 ml of sterile RPMI 1640 medium. The peritoneal fluid was carefully aspirated avoiding hemorrhage and kept at 4°C to prevent the adhesion of the macrophages to the plastic. An aliquot of the cell suspension was used to determine the cell density in the peritoneal fluid. The cells were centrifuged at 200**g** for 10 min at 4°C and the pellet was washed twice with 25 ml of ice-cold PBS. Cells were seeded at $1x10^6/cm^2$ in RPMI 1640 medium supplemented with 10% of heat inactivated FCS and antibiotics. After incubation for 3 h at 37°C in a 5% CO_2 atmosphere, non-adherent cells were removed by extensive washing with PBS. Experiments were carried out in phenol-red free RPMI 1640 medium and 1% of heat inactivated FCS plus antibiotics (13). Prior to stimulation, the medium was aspirated and replaced by warm medium containing the indicated TLR ligand or cytokine. When the murine macrophage RAW 264.7 cells were used, they were processed as indicated for the peritoneal macrophages.

Flow cytometry. Cells were harvested and washed in cold phosphate-buffered saline (PBS). After centrifugation at 4ºC for 5 min and 1000**g**, cells were resuspended in annexin V binding buffer (10 mM HEPES; pH 7.4, 140 mM NaCl, 2.5 mM $CaCl_2$). Cells were labeled with annexin V–FITC solution and/or propidium iodide (PI) (100 µg/ml) for 15 min at RT in the dark. PI is impermeable to living and apoptotic cells but stains necrotic and apoptotic dying cells with impaired membrane integrity in contrast to annexin V, which stains early apoptotic cells.

Assay of PFK-2 activity. Cultured macrophages (6 cm dishes) were homogenized in 1 ml of a medium containing 20 mM potassium phosphate (pH 7.4, 4°C), 1 mM DTT, 50 mM NaF, 0.5 phenylmethanesulphonyl fluoride, 10 µM leupeptin and 5 % poly(ethylene)glycol. After centrifugation in an Eppendorf centrifuge (15 min), poly(ethylene)glycol was added to the supernatant up to 15 % (mass:vol) to fully precipitate the PFK-2. After resuspension of the pellet in the extraction medium, PFK-2 activity was assayed at pH 8.5 with 5 mM

MgATP and 5 mM Fru-6-phosphate, 15 mM Glc-6-phosphate. One unit of PFK-2 activity is the amount of enzyme that catalyzes the formation of one pmol of Fru-2,6-P_2 per min (14).

Metabolite assays. Fru-2,6-P_2 was extracted from cells (24-well plates) after homogenization in 100 µl of 50 mM NaOH followed by heating at 80ºC for 10 min. The metabolite was measured by the activation of the PPi-dependent phosphofructo-1-kinase (14). Lactate and glucose were measured enzymically in the culture medium. NO release was determined spectrophotometrically by the accumulation of nitrite and nitrate in the medium (phenol red-free). Nitrate was reduced to nitrite, and this was determined with Griess reagent (13) by adding 1 mM sulfanilic acid and 100 mM HCl (final concentration). After a first reading of the absorbance at 548 nm, naphthylenediamine (1 mM in the assay) was added and the absorbance was compared with a standard of $NaNO_2$. Results were expressed as the amount of nitrite and nitrate released per mg of cell protein.

Cytokine assay. The accumulation of TNF-α and IL-6 was measured per triplicate using commercial kits (Biotrak, GE Healthcare), following the indications of the supplier.

Preparation of cell extracts. The macrophage cultures (6-well dishes) were washed twice with ice-cold PBS and the cells were homogenized in 0.2 ml of buffer containing 10 mM Tris-HCl, pH 7.5, 1 mM $MgCl_2$, 1 mM EGTA, 10% glycerol, 0.5% CHAPS, 1 mM β-mercaptoethanol and 0.1 mM PMSF and a protease inhibitor cocktail (Sigma). The extracts were vortexed for 30 min at 4ºC and centrifuged for 20 min at 13000**g**. The supernatants were stored at -20ºC. Proteins levels were determined using the Bio-Rad detergent-compatible protein reagent (Richmond, CA). All steps were carried out at 4ºC.

Western blot analysis. Samples of cell extracts containing equal amounts of protein (30 µg per lane) were boiled in 250 mM Tris-HCl, pH 6.8, 2% SDS, 10% glycerol, 2% β-mercaptoethanol and size-separated in 10% SDS-PAGE. The gels were blotted onto a PVDF membrane (GE Healthcare, UK) and processed as recommended by the supplier of the antibodies against the murine antigens: NOS-2 (sc-7271), COX-2 (sc-1999), MHC-II (sc-59322), HO-1 (AB-1284), Arg-1 (sc-20150), SOCS3 (2923s), KC/CXCL1 (AF-453-NA), IP-10/CXCL10 (500-p129), L-PFK-2 (sc-10096) and actin (A-5441). For uPFK-2, specific peptides of the isoenzyme were used to generate polyclonal antibodies by immunization of rabbits (New Zealand White) with multiple intradermal injections with 300 µg of antigen in 1 ml of complete Freund's adjuvant, followed by boosters with 100 µg of antigen in incomplete Freund's adjuvant. The blots were developed by ECL protocol (Amersham) and different exposition times were performed for each blot with a charged coupling device camera in a luminescent image analyzer (Molecular Imager, BioRad) to ensure the linearity of the band intensities.

Microarray analysis. Normalized expression data were obtained from NCBI GEO dataset GDS2429 (15) using GEOquery package from Bioconductor (16). Differential expression for the following comparisons was tested using limma Bioconductor package (17): a) naïve mature macrophage *vs.* classic activated macrophage and, b) alternatively activated macrophage. Two gene lists were generated after each comparison and they were ranked according to the test statistic for subsequent Gene Set Enrichment Analysis (GSEA). Enrichment of gene sets of interest in each list was accomplished using the GSEA method as described by Mootha et al. (18). We used "Which genes?" (http://www.whichgenes.org/) to retrieve the REACTOME (19) pathways as gene sets. The genes from the two lists were also mapped into canonical pathways using Ingenuity Pathway Analysis software (Ingenuity Systems, see Supplementary material).

GCMS sample preparation and procedure. The macrophages cultures (10 cm dishes) were washed twice with ice-cold PBS and culture media was replaced by 50% enriched [1,2-$^{13}C_2$]-glucose containing the indicated TLR ligand or cytokine. At the end of the incubations, cells were centrifuged (200**g** for 5 min) and incubation medium and cell pellets were obtained and store at -80ºC until processing. Glucose, lactate, glutamine and glutamate incubation medium concentrations were determined as previously described (20, 21) using a Cobas Mira Plus chemistry analyzer (HORIBA ABX, Montpelier, France). Lactate from the cell culture media was extracted by ethyl acetate after acidification with HCl. Lactate was derivatized to its propylamide-heptafluorobutyric form and the *m/z* 328 (carbons 1-3 of lactate, chemical ionization) was monitored for the detection of m1 (lactate with a [^{13}C] in one position) and m2 (double-labeled lactate) for the estimation of pentose cycle activity versus anaerobic glycolysis (22). RNA ribose was isolated by acid hydrolysis of cellular RNA after Trizol-purification of cell extracts. Ribose isolated from RNA was derivatized to its aldonitrile acetate form using hydroxylamine in pyridine and acetic anhydride. We monitored the ion cluster around the *m/z* 256 (carbons 1-5 of ribose, chemical ionization), in order to find the molar enrichment of [^{13}C] labels in ribose (22). Glutamate was separated from the medium using ion-exchange chromatography (23). Glutamate was converted to its n-trifluoroacetyl-n-butyl derivative and the ion clusters *m/z* 198 (carbons 2-5 of glutamate, electron impact ionization) and *m/z* 152 (carbons 2-4 of glutamate, electron impact ionization) were monitored. Isotopomeric analysis of C2-C5 and C2-C4 fragments of medium glutamate was done in order to estimate the relative contributions of pyruvate carboxylase and pyruvate dehydrogenase to the Krebs cycle (24, 25). Mass spectral data were obtained on the QP2010 Shimadzu mass selective detector connected to a GC-2010 gas chromatograph. The settings were as follows: GC inlet for glucose and ribose 250ºC and 200ºC for lactate and glutamate, transfer line 250ºC, MS source 200ºC. A Varian VF-5 capillary column (30-m length, 250-mm diameter, 0.25-mm film thickness) was used to analysis of all compounds studied.

Statistical analysis. The data shown are the means ± SD of three or four experiments. Statistical significance was estimated with Student's *t* test for unpaired observations. A *P* value of less than 0.05 was considered significant.

Results

Distribution of substrate fluxes in activated macrophages. Elicited peritoneal macrophages were isolated and maintained in culture for the indicated periods of time. After overnight seeding, cells were activated through TLRs involved in innate immunity (TLR4: LPS; TLR2: LTA; TLR3: polyI·C and TLR9: CpG), classic activation (LPS/IFN-γ) and alternative pathway (IL-4/IL-13; IL10) (5, 6). Fig. 1A shows the expression of a panel of representative markers of macrophage activation. NOS-2 and COX-2 were expressed similarly in cells activated through the innate and classic response, except through CpG stimulation. MHC-II up-regulation was very sensitive to LPS signaling and to the classic activation pathway and arginase-1 was notably up-regulated in response to IL-4/IL-13. Hemeoxygenase-1 was moderately induced by innate and alternative pathways of activation. SOCS3 was up-regulated in response to LPS or LPS/IFN-γ. The chemokine CXCL1/KC was expressed in cells activated through classic signaling pathway and innate immunity mediated by TLR2 and TLR4 and CXCL10/IP-10 was up-regulated through the classic and the innate response. In addition to these parameters characteristic of macrophage activation, cell viability was determined: apoptosis was evaluated by annexin V exposure of the cells and by positivity for PI labeling, the later characteristic of dying cells. As Fig. 1B shows, an increase of annexin V was observed in cells treated with LPS/IFN-γ, and to a lesser extent with LPS; however, the percentage of PI positive cells at this time (12h) was modest suggesting that the integrity of the plasma membrane remained preserved. These data were reminiscent of the expression of NOS-2 indicating that NO plays an important role in the induction of apoptosis in these cells (not shown, (26)). Staurosporine was used as a reference for apoptosis induction in macrophages. Moreover, the accumulation in the culture medium of IL-6, TNF-α and nitrites/nitrates indicated the activation by ligands, such as CpG that fails to promote NOS-2 expression but increased IL-6 and TNF-α synthesis (Fig. 1C).

Previous data suggested the relevance of carbohydrate metabolism in the commitment for activation of macrophages (27-30). In this regard, we investigated the glucose consumption and fate in macrophages activated through the innate, classic and alternative pathways. As Fig. 2 shows, two clear profiles were observed in terms of glucose consumption and lactate release: TLR activation promoted an enhancement in the glycolytic flux to lactate that has temporally dependent profiles, but can be grouped into two categories: one from 0 to 4h and a second flux rate between 4 and 12h. Indeed, when the same experiment was performed with [1,2-$^{13}C_2$]-glucose, the distribution of [^{13}C]-glucose metabolites, according to the scheme depicted in Fig. 3, allowed the measurement of the precise contribution of these time-dependent fluxes in activated macrophages. From 0 to 4h the glycolytic activity was much lower than from 4 to 12h (Fig. 4A). Interestingly, stimulation through the alternative pathway, despite to influence the expression of a specific set of genes (*vide infra*), exhibited a metabolic profile that essentially matched that of control cells. Also, and in agreement with previous work, macrophages displayed a metabolic flux that involved the conversion of

glucose into lactate by more than 95%, regardless the activation pathway considered (Fig. 4B). The metabolic features revealed by glucose consumption and lactate release are followed by a basal consumption of glutamine and glutamate production (Fig. 2). Besides, low enrichment in glutamate and RNA (Fig. 4B and 5B) evidenced the high glycolytic pattern in peritoneal macrophages. Peritoneal macrophages are quiescent cells; however, when the macrophage cell line RAW 264.7 cells was used and kept overnight with 1% FCS, stimulation after 12h under these conditions revealed that the basal proliferation rate of these cells did not influence the metabolic profile associated to the macrophage activation process. As Fig. 5A shows, RAW 264.7 cells follow a similar mass isotope distribution in lactate than peritoneal macrophages under basal conditions. However, proliferation induces higher metabolic fluxes and [^{13}C] enrichment in ribose and glutamate (Fig. 5B).

Gene profiling in stimulated macrophages. The previous experiments showed that carbohydrate metabolism in macrophages is fundamentally glycolytic and that the rate of glucose consumption is lower in alternatively activated macrophages than in classic activation. We hypothesized that the expression levels of genes involved in energetic pathways may differ between the two types of macrophage activation. To test this hypothesis we compared the functional enrichment (in up or down-regulated genes) of the following REACTOME (19) pathways: "Glycolysis", "Pyruvate metabolism and TCA cycle" and "Electron Transport Chain". Glycolysis was enriched in up-regulated genes of classic activation (False Discovery Rate, FDR, 0.32; Fig. 6A). There was a similar enrichment trend of glycolysis in alternative activation but it was not significant (FDR 0.547, Fig. 6A and Supp.1). Moreover, pyruvate metabolism and TCA cycle pathways were most clearly enriched in up-regulated genes during alternative activation (FDR 0.097) whereas the opposite trend was observed for the classic macrophage activation although statistically not significant (FDR 0.455) (Fig. 6A and Supp. 2). Noteworthy, the most significant enrichment (FDR 0.000) was found in genes down-regulated during classic activation, an effect not observed for the alternative activation (Fig. 6A and Supp.3). These data suggest that classic activation has a stronger effect on the gene expression of genes related with the energetic metabolism, favoring the up-regulation of genes from the glycolytic pathway and repression of genes encoding for proteins that participate in the oxidative phosphorylation.

PFK-2/FBPase-2 isoenzyme changes in activated macrophages. The aforementioned differences in transcription of the glycolysis gene-set between classic and alternative activation of macrophages allowed us hypothesize that PFK-2, one of the key enzymes of the pathway, could be regulated at the protein and/or enzymatic level. Accordingly, the expression of the isoforms of PFK-2 and the levels of Fru-2,6-P_2 were determined under these conditions as an indication of the capacity of these cells to metabolize glucose (14, 31). As Fig. 6B shows, resting macrophages expressed the L-type isoenzyme of PFK-2, but not the uPFK-2

isoenzyme, resulting in low steady state levels of Fru-2,6-P_2. However, as result of the activation through the classic and innate pathway, but not the alternative pathway, a robust expression of the uPFK-2 isoenzyme occurred, concomitant with an up to 9-fold rise in the PFK-2 activity and 5-fold increase in the levels of Fru-2,6-P_2. Interestingly, the levels of expression of uPFK2, and more importantly, the enzyme activity and intracellular concentration of Fru-2,6-P_2 exhibited parallel profiles for each activation condition. Moreover, neither IL-4, IL-10 nor IL-13 were able to change the expression pattern of PFK-2 nor to increase Fru-2,6-P_2 levels. To evaluate the capacity of these IL to influence the response to LPS co-stimulation studies were done. As Fig. 6C shows, when combined IL-10 and IL-4 with LPS, the intracellular levels of Fru-2,6-P_2 were only minimally influenced with respect to the LPS condition and an important expression of uPFK-2 occurred, despite to maintain a certain level of L-PFK-2 expression.

Discussion

Previous work established that peritoneal macrophages are essentially glycolytic cells (10, 11, 28, 29, 32, 33). Compared with other cell types macrophages use mainly anaerobic glycolysis in the metabolization of glucose, and the measured flux in isolated cells is ca. 10% of the actual capacity through 6-phosphofructo-1-kinase, one of the enzymes that controls the glycolytic pathway (29). In addition to this, glutamine is converted into glutamate and aspartate and less than 10% is being oxidized, at the time that fatty acids appear to be the main substrates for oxidative metabolism (28). In the present work, it has been assessed the metabolic profiles associated to stimulation of macrophages through three well-defined activation-pathways, using a metabolomic approach. The data obtained show that regardless the stimulation pathway involved, macrophages remain glycolytic cells and accelerate notably the conversion of glucose into lactate when challenged through the classic/innate activation pathways; however, the activation through the alternative pathway exerted minimal effects on the basal consumption of glucose. One of the relevant regulators of glucose metabolism is the rise in the levels of Fru-2,6-P_2 that in turn activates the flux through 6-phosphofructo-1-kinase (30, 34, 35). Fru-2,6-P_2 is synthesized/degraded by PFK-2/FBPase-2 activities. Four genes encode the PFK-2 in higher mammals. The L-type is encoded by the *PFKB1* gene and is mainly expressed in liver and a splicing variant is expressed in muscle. This enzyme has a balanced kinase/bisphosphatase ratio and unless the bisphosphatase activity is inhibited, it maintains low levels of Fru-2,6-P_2 through a futile cycle of synthesis and degradation of the metabolite (34, 35). The uPFK-2 encoded by the *PFKB3* gene has a higher kinase activity (ca. 10:1 kinase:bisphosphatase), is induced by hypoxia and can be regulated by phosphorylation, playing a role in the high glycolytic rate of various cell types, such as cancer cells (30, 36-38). A relevant finding of this work is the observation that concomitant to the classic/innate activation there is a switch in the expression of the PFK-2/FBPase-2 from the L-type to the uPFK-2 isoenzyme. Interestingly, this form exhibits a higher capacity to accumulate Fru-2,6-P_2 in macrophages, due to its lower bisphosphatase activity compared with the L-type, which results in an enhancement in the levels of Fru-2,6-P_2 at the time that there is an increase in the enzymatic activity determined *in vitro* and in the glycolytic flux. Moreover, it is remarkable the substitutions between the two isoenzymes and, in fact, the protein levels of L-PFK-2 almost disappear and are substituted by the uPFK-2 in the course of TLR-2, -3, -4 or -9 activation, despite the use of non-redundant signaling pathways; i.e. MyD88 dependent and independent pathways. This switch between PFK-2 isoenzymes is absent in macrophages activated through the alternative pathway and studies on the molecular basis of this transcriptional control are in progress. Regarding the mass isotopomer distribution in both resting and activated macrophages, the distribution of the label is essentially identical confirming the minor impact of cell activation among switching between glucose fueling pathways. Although the three activation pathways studied involve

changes in the expression of a large number of genes, the present work shows that only classic and innate activation through TLRs results in an enhanced expression of PKFB3 corresponding to a higher activation of PFK-2 activity and glycolytic flux. These results correlate with model flux predictions in LPS stimulated RAW 264.7 cells [Rodriguez-Prados et al, unpublished]. This model could estimate the central metabolism flux distribution from [^{13}C] labeling data and metabolites consumption and production rates.

This metabolic effect upon macrophage challenge is observed both in proliferating (the RAW 264.7 cells) and non-proliferating cells (elicited peritoneal macrophages). However, our results highlight that proliferation has a higher effect on metabolism than the one induced by the activation process. Therefore, metabolic changes strictly associated to macrophage activation correspond to results observed in peritoneal macrophages experiments. Metabolic differences induced by proliferation are shown in Fig. 5B. RAW 264.7 have higher metabolic fluxes than peritoneal macrophages. Besides, as expected, [^{13}C] enrichment in ribose and glutamate are higher in RAW 264.7 to cover the demand in metabolites to form new cells. Moreover, the higher flux through pentose phosphate pathway (PPP) to synthesize nucleotides results in a higher label in m1 lactate due to the recycling through the non-oxidative branch of PPP (Figs. 4B and 5A). Finally, the lower glycolytic flux in RAW 264.7 indicates that proliferation promotes the recruitment of other carbon source like glutamine in an anaplerotic flux, corroborating the role of glutamine metabolism in macrophage activation already described (9).

In conclusion the data show that the stimulation of macrophages through the classic, innate and alternative pathways exhibits, as expected, a distinctly expression of activation markers due to different signaling events involved in each pathway. However, the innate pathway activation shows a higher glycolytic rate due to a switch in the expression of PFK-2 isoenzymes that appears to be a common event after LPS/IFNγ or TLR-2, -3, -4 -9 stimualtion. Despite the differences in glucose consumption and lactate release, label distribution analysis shows that there is a common metabolic pattern followed regardless the activation pathway.

Acknowledgments

We thank Dr Simon Bartlett for the discussion, advice and critical reading of the manuscript. The authors thank Dr Ramón Bartrons (Universitat de Barcelona, Spain) for the generous gift of the uPFK-2 Ab.

Abbreviations

Arg-1, Arginase-1; COX-2, Cyclooxygenase-2; CpG, Cytosine Guanine dinucleotide; GCMS, Gas Chromatography/Mass Spectrometry; g3p, glyceraldehyde-3-phosphate; HO-1, Hemeoxygenase-1; IFN-γ, Interferon-γ; IL-4/10/13, Interleukin-4/10/13; IP-10/CXCL10, Chemokine (C-X-C motif) ligand 10; KC/CXCL1, Chemokine (C-X-C motif) ligand 1; LDL, Low Density Lipoprotein; LPS, Lipopolysaccharide; LTA, Lipoteichoic Acid; NOS-2, Nitric Oxide Synthase-2; MHC-II, Major Histocompatibility Complex-II; MIDA, Mass Isotopomer Distribution Analysis; PAMPs, Pathogen-Associated Molecular Patterns; PFK-2/FBPase-2, 6-phosphofructo-2-kinase (EC 2.7.1.105)/fructose-2,6-bisphosphatase (EC 3.1.3.46); PPP, Pentose Phosphate Pathway; PRRs, Pattern-Recognition Receptors; polyI·C, polyriboinosinic:polyribocytidylic acid; PVDF, Polyvinylidene Fluoride; ROS, Reactive Oxygen Species; SDS-PAGE, Sodium Dodecyl Sulphate Polyacrylamide gel electophoresis; SOCS3, Suppressor Of Cytokine Signaling-3; TLRs, Toll-Like Receptors; TGF-β, Transforming Growth Factor-β ; TNF-α, tumor Necrosis Factor-α.

References

1. Gordon, S., C. Pasare, and R. Medzhitov. 2007. The macrophage: past, present and future. Toll-like receptors: linking innate and adaptive immunity. *Eur J Immunol* 37 Suppl 1:S9-17.
2. Pasare, C., and R. Medzhitov. 2004. Toll-like receptors: linking innate and adaptive immunity. *Microbes Infect* 6:1382-1387.
3. Lombardo, E., A. Alvarez-Barrientos, B. Maroto, L. Bosca, and U. G. Knaus. 2007. TLR4-mediated survival of macrophages is MyD88 dependent and requires TNF-α autocrine signalling. *J Immunol* 178:3731-3739.
4. Bosca, L., M. Zeini, P. G. Traves, and S. Hortelano. 2005. Nitric oxide and cell viability in inflammatory cells: a role for NO in macrophage function and fate. *Toxicology* 208:249-258.
5. Gordon, S., and P. R. Taylor. 2005. Monocyte and macrophage heterogeneity. *Nat Rev Immunol* 5:953-964.
6. Mantovani, A., A. Sica, and M. Locati. 2005. Macrophage polarization comes of age. *Immunity* 23:344-346.
7. Wolowczuk, I., C. Verwaerde, O. Viltart, A. Delanoye, M. Delacre, B. Pot, and C. Grangette. 2008. Feeding our immune system: impact on metabolism. *Clin Dev Immunol* 2008:639803.
8. Matarese, G., and A. La Cava. 2004. The intricate interface between immune system and metabolism. *Trends Immunol* 25:193-200.
9. Newsholme, P. 2001. Why is L-glutamine metabolism important to cells of the immune system in health, postinjury, surgery or infection? *J Nutr* 131:2515S-2522S; discussion 2523S-2514S.
10. Bustos, R., and F. Sobrino. 1992. Stimulation of glycolysis as an activation signal in rat peritoneal macrophages. Effect of glucocorticoids on this process. *Biochem J* 282:299-303.
11. Wu, G. Y., C. J. Field, and E. B. Marliss. 1991. Glucose and glutamine metabolism in rat macrophages: enhanced glycolysis and unaltered glutaminolysis in spontaneously diabetic BB rats. *Biochim Biophys Acta* 1115:166-173.
12. Cascante, M., and S. Marin. 2008. Metabolomics and fluxomics approaches. *Essays Biochem* 45:67-81.
13. Velasco, M., M. J. Diaz-Guerra, P. Diaz-Achirica, D. Andreu, L. Rivas, and L. Bosca. 1997. Macrophage triggering with cecropin A and melittin-derived peptides induces type II nitric oxide synthase expression. *J Immunol* 158:4437-4443.
14. Martin-Sanz, P., M. Cascales, and L. Bosca. 1989. Glucagon-induced changes in fructose 2,6-bisphosphate and 6-phosphofructo-2-kinase in cultured rat foetal hepatocytes. *Biochem J* 257:795-799.
15. Martinez, F. O., S. Gordon, M. Locati, and A. Mantovani. 2006. Transcriptional profiling of the human monocyte-to-macrophage differentiation and polarization: new molecules and patterns of gene expression. *J Immunol* 177:7303-7311.
16. Gentleman, R. C., V. J. Carey, D. M. Bates, B. Bolstad, M. Dettling, S. Dudoit, B. Ellis, L. Gautier, Y. Ge, J. Gentry, K. Hornik, T. Hothorn, W. Huber, S. Iacus, R. Irizarry, F. Leisch, C. Li, M. Maechler, A. J. Rossini, G. Sawitzki, C. Smith, G. Smyth, L. Tierney, J. Y. Yang, and J. Zhang. 2004. Bioconductor: open software development for computational biology and bioinformatics. *Genome Biol* 5:R80.
17. Smyth, G. K. 2004. Linear models and empirical bayes methods for assessing differential expression in microarray experiments. *Stat Appl Genet Mol Biol* 3:Article3.
18. Mootha, V. K., C. M. Lindgren, K. F. Eriksson, A. Subramanian, S. Sihag, J. Lehar, P. Puigserver, E. Carlsson, M. Ridderstrale, E. Laurila, N. Houstis, M. J. Daly, N. Patterson, J. P. Mesirov, T. R. Golub, P. Tamayo, B. Spiegelman, E. S. Lander, J. N. Hirschhorn, D. Altshuler, and L. C. Groop. 2003. PGC-1alpha-responsive genes involved in oxidative phosphorylation are coordinately downregulated in human diabetes. *Nat Genet* 34:267-273.
19. Matthews, L., G. Gopinath, M. Gillespie, M. Caudy, D. Croft, B. de Bono, P. Garapati, J. Hemish, H. Hermjakob, B. Jassal, A. Kanapin, S. Lewis, S. Mahajan, B. May, E. Schmidt, I. Vastrik, G. Wu, E. Birney, L. Stein, and P. D'Eustachio. 2009. Reactome knowledgebase of human biological pathways and processes. *Nucleic Acids Res* 37:D619-622.
20. Gutmann, I., and A. W. Wahlefeld. 1974. L-(+)-Lactate determination with lactate dehydrogenase and NAD. In *Methods in Enzymatic Analysis*, 2nd ed. H. U. Bergmeyer, J. Bergmeyer, and M. Grassl, eds. Academic, New York. 1464-1468.

21. Kunst, A., B. Draeger, and J. Ziegenhorn. 1984. D-Glucose. UV-methods with hexokinase. In *Methods of Enzymatic Analysis*, 3rd ed. H. U. Bergmeyer, J. Bergmeyer, and M. Grassl, eds. Verlag Chemie, Weinheim. 163-172.
22. Lee, W. N., L. G. Boros, J. Puigjaner, S. Bassilian, S. Lim, and M. Cascante. 1998. Mass isotopomer study of the nonoxidative pathways of the pentose cycle with [1,2-13C2]glucose. *Am J Physiol* 274:E843-851.
23. Katz, J., W. N. Lee, P. A. Wals, and E. A. Bergner. 1989. Studies of glycogen synthesis and the Krebs cycle by mass isotopomer analysis with [U-^{13}C]glucose in rats. *J Biol Chem* 264:12994-13004.
24. Boros, L. G., M. Cascante, and W. N. Lee. 2002. Metabolic profiling of cell growth and death in cancer: applications in drug discovery. *Drug Discov Today* 7:364-372.
25. Lee, W. N., J. Edmond, S. Bassilian, and J. W. Morrow. 1996. Mass isotopomer study of glutamine oxidation and synthesis in primary culture of astrocytes. *Dev Neurosci* 18:469-477.
26. Hortelano, S., P. G. Traves, M. Zeini, A. M. Alvarez, and L. Bosca. 2003. Sustained nitric oxide delivery delays nitric oxide-dependent apoptosis in macrophages: contribution to the physiological function of activated macrophages. *J Immunol* 171:6059-6064.
27. Newsholme, P., and E. A. Newsholme. 1989. Rates of utilization of glucose, glutamine and oleate and formation of end-products by mouse peritoneal macrophages in culture. *Biochem J* 261:211-218.
28. Newsholme, P., S. Gordon, and E. A. Newsholme. 1987. Rates of utilization and fates of glucose, glutamine, pyruvate, fatty acids and ketone bodies by mouse macrophages. *Biochem J* 242:631-636.
29. Newsholme, P., R. Curi, S. Gordon, and E. A. Newsholme. 1986. Metabolism of glucose, glutamine, long-chain fatty acids and ketone bodies by murine macrophages. *Biochem J* 239:121-125.
30. Bando, H., T. Atsumi, T. Nishio, H. Niwa, S. Mishima, C. Shimizu, N. Yoshioka, R. Bucala, and T. Koike. 2005. Phosphorylation of the 6-phosphofructo-2-kinase/fructose 2,6-bisphosphatase/PFKFB3 family of glycolytic regulators in human cancer. *Clin Cancer Res* 11:5784-5792.
31. Cascales, M., P. Martin-Sanz, and L. Bosca. 1992. Phorbol esters, bombesin and insulin elicit differential responses on the 6-phosphofructo-2-kinase/fructose-2,6-bisphosphatase system in primary cultures of foetal and adult rat hepatocytes. *Eur J Biochem* 207:391-397.
32. Albina, J. E., and B. Mastrofrancesco. 1993. Modulation of glucose metabolism in macrophages by products of nitric oxide synthase. *Am J Physiol* 264:C1594-1599.
33. Mateo, R. B., J. S. Reichner, B. Mastrofrancesco, D. Kraft-Stolar, and J. E. Albina. 1995. Impact of nitric oxide on macrophage glucose metabolism and glyceraldehyde-3-phosphate dehydrogenase activity. *Am J Physiol* 268:C669-675.
34. Okar, D. A., A. Manzano, A. Navarro-Sabate, L. Riera, R. Bartrons, and A. J. Lange. 2001. PFK-2/FBPase-2: maker and breaker of the essential biofactor fructose-2,6-bisphosphate. *Trends Biochem Sci* 26:30-35.
35. Rider, M. H., L. Bertrand, D. Vertommen, P. A. Michels, G. G. Rousseau, and L. Hue. 2004. 6-phosphofructo-2-kinase/fructose-2,6-bisphosphatase: head-to-head with a bifunctional enzyme that controls glycolysis. *Biochem J* 381:561-579.
36. Calvo, M. N., R. Bartrons, E. Castano, J. C. Perales, A. Navarro-Sabate, and A. Manzano. 2006. PFKFB3 gene silencing decreases glycolysis, induces cell-cycle delay and inhibits anchorage-independent growth in HeLa cells. *FEBS Lett* 580:3308-3314.
37. Minchenko, A., I. Leshchinsky, I. Opentanova, N. Sang, V. Srinivas, V. Armstead, and J. Caro. 2002. Hypoxia-inducible factor-1-mediated expression of the 6-phosphofructo-2-kinase/fructose-2,6-bisphosphatase-3 (PFKFB3) gene. Its possible role in the Warburg effect. *J Biol Chem* 277:6183-6187.
38. Obach, M., A. Navarro-Sabate, J. Caro, X. Kong, J. Duran, M. Gomez, J. C. Perales, F. Ventura, J. L. Rosa, and R. Bartrons. 2004. 6-Phosphofructo-2-kinase (pfkfb3) gene promoter contains hypoxia-inducible factor-1 binding sites necessary for transactivation in response to hypoxia. *J Biol Chem* 279:53562-53570.

Legends to Figures.

Fig. 1. ***Characterization of macrophages stimulated through the classic, innate and alternative pathways.*** Peritoneal macrophages were maintained in culture and stimulated with the indicated stimuli: LPS/IFN-γ (250 ng/ml and 20 ng/ml, respectively); LPS (100 ng/ml); IL-13, IL-4, IL-10 (20 ng/ml each); LTA (5 μg/ml); polyI·C (25 μg/ml); CpG (3 μg/ml); staurosporine (100 ng/ml). The levels of the indicated proteins were determined by Western blot (panel A). The extent of apoptosis/necrosis was determined by the staining with annexin V/propidium iodide, respectively (panel B). The release of IL-6, TNF-α, and nitrite/nitrate to the culture medium was determined as described in the methods section (C). Results show the mean ± SD of five experiments. *P<0.01 *vs.* the vehicle condition.

Fig. 2. ***Metabolic fluxes in macrophages stimulated though the classic, innate and alternative pathways.*** The time course of glucose and glutamine consumption and lactate and glutamate release were determined enzymically by sampling the culture medium at periods of 2 h. Results show the mean of five experiments.

Fig. 3. ***Schematic representation of tracer-based determination of metabolic fluxes.*** Macrophages were loaded with [1,2-$^{13}C_2$]-glucose and the [^{13}C] trace was followed by GCMS to establish unambiguously the fate of glucose in cells stimulated through the classic, innate and alternative pathways. [1,2-$^{13}C_2$]-glucose could follow the oxidative branch of pentose phosphate pathway to provide [1-$^{13}C_1$]-ribose (== line) or the upper part of glycolysis driving to the [1,2-$^{13}C_2$]-g3p formation (▬ line). Recycling through the non-oxidative branch of pentose phosphate pathway allows the formation of [1-$^{13}C_1$]-g3p and [1,2-$^{13}C_2$]-ribose, respectively. Label pattern does not change in the lower part of glycolysis and the lactate formed could drive into the four depicted isotopomers of glutamate depending on whether pyruvate dehydrogenase or pyruvate carboxykinase is used to enter in the Krebs cycle.

Fig. 4. ***Metabolic fluxes using tracer-based distribution of [^{13}C] in stimulated macrophages.*** Peritoneal macrophages were maintained in culture and stimulated for 12h in the presence of [1,2-$^{13}C_2$]-glucose as indicated in Fig. 1. Samples of culture medium were collected at 4h and 12h and the distribution of the [^{13}C] label was determined by GCMS to establish the metabolic fluxes (panel A). The distribution of the label for m0, m1 and m2 lactate at 12h is shown (panel B). Results show the mean ± SD of four experiments. *P<0.01 *vs.* the vehicle condition.

Fig. 5. ***Metabolic fluxes using tracer-based distribution of [^{13}C] in stimulated RAW264.7 cells.*** The macrophage cell line was maintained overnight with 1% FCS and stimulated for 12h in the presence of [1,2-$^{13}C_2$]-glucose as indicated in Fig. 1 for peritoneal macrophages. Samples of culture medium were collected at 6h and 12h and the distribution of the [^{13}C] label in lactate was determined by GCMS to establish the metabolic fluxes (panel A). The comparison between peritoneal macrophages and the RAW 264.7 cell line of the main metabolic fluxes and [^{13}C] enrichment in ribose and glutamate is shown in panel B. Results show the mean ± SD of four experiments. *P<0.0051 *vs.* peritoneal macrophages.

Fig. 6. ***Gene Set Enrichment Analysis (GSEA) of energy metabolism pathways and PFK-2/FBPase-2 isoenzyme switch in activated macrophages.*** The Normalized Enriched Score (NES) calculated by GSEA is shown in the bars, and numbers indicate the False Discovery Rate (FDR) for the enrichment. Positive NES indicates enrichment in up-regulated genes while negative NES correspond to enrichment in down-regulated genes. See Supplementary material for more details (panel A). Peritoneal macrophages were maintained in culture and stimulated for 12h as indicated in Fig. 1. The levels of the L-PFK-2 and uPFK-2 isoenzymes were determined by Western blot using specific antibodies. Cell extracts were prepared and the activity of PFK-2 was determined in vitro. The levels of Fru-2,6-P_2 were determined in cell extracts after collection of the cell pellets in 50 mM NaOH at 80ºC (panel B). Co-treatment of cells with LPS and IL-10 or IL-4 results in a decrease in Fru-2,6-P_2 content (panel C). Results show the mean ± SD of five experiments. *P<0.01 *vs.* the vehicle condition; #P<0.05 *vs.* the LPS condition (panel C).

Supplementary material

The gene lists (1) classic activation and (2) alternative activation of macrophage were generated and analyzed as described in the Methods section of the manuscript. Here we show the enrichment plots from Gene Set Enrichment Analysis (GSEA) for the three REACTOME pathways analyzed, together with the genes mapped into canonical pathways generated by Ingenuity Pathway Analysis software (Ingenuity

Systems). GSEA enrichment plots show up-regulated genes in red and down-regulated genes in blue. In contrast, down-regulated genes in Ingenuity pathways are in green. There are three supplementary figures:
Supp. 1. Glycolysis.
Supp. 2. Pyruvate metabolism and TCA cycle.
Supp. 3. Electron Transport Chain.

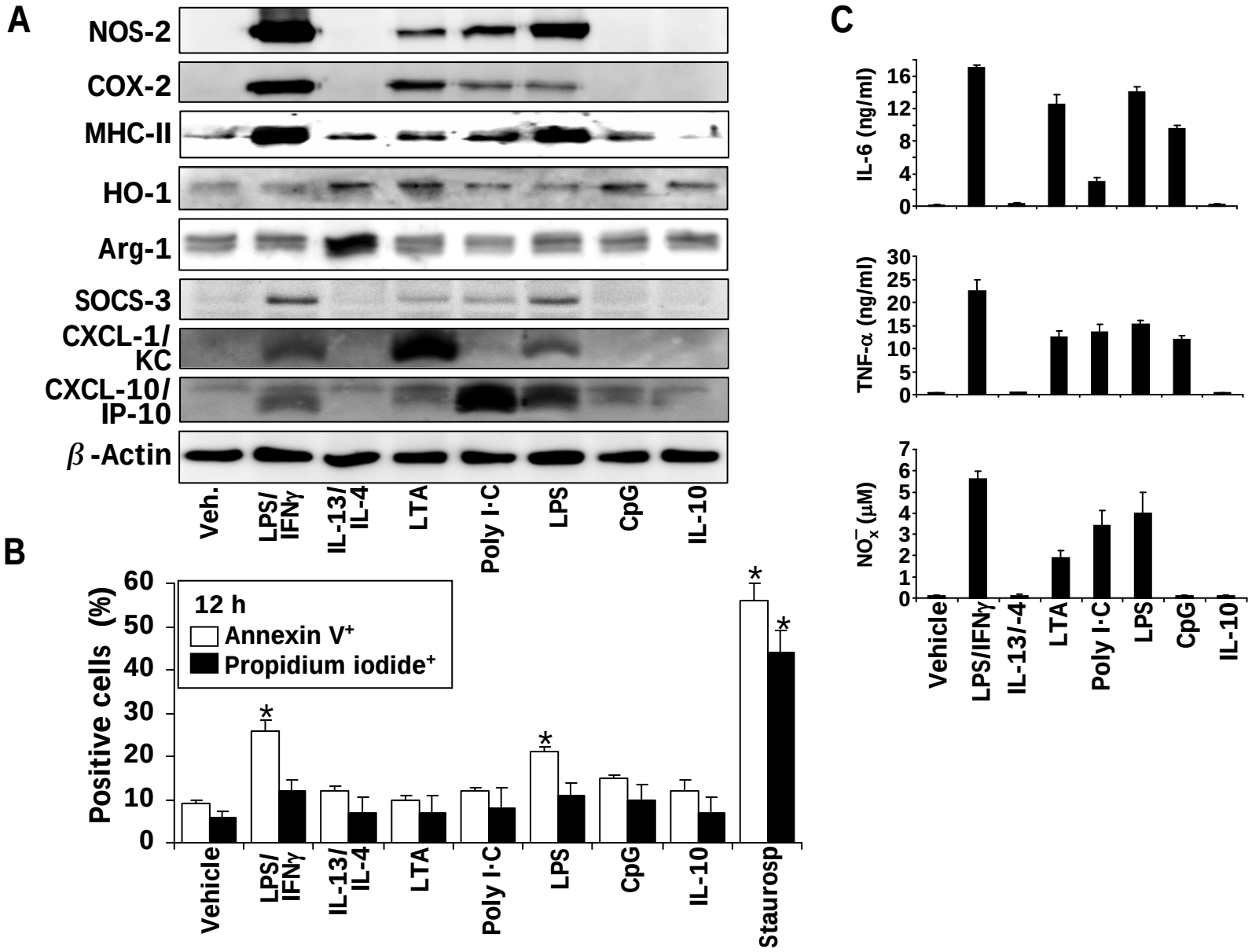

Fig. 1
Rod-Prados et al.

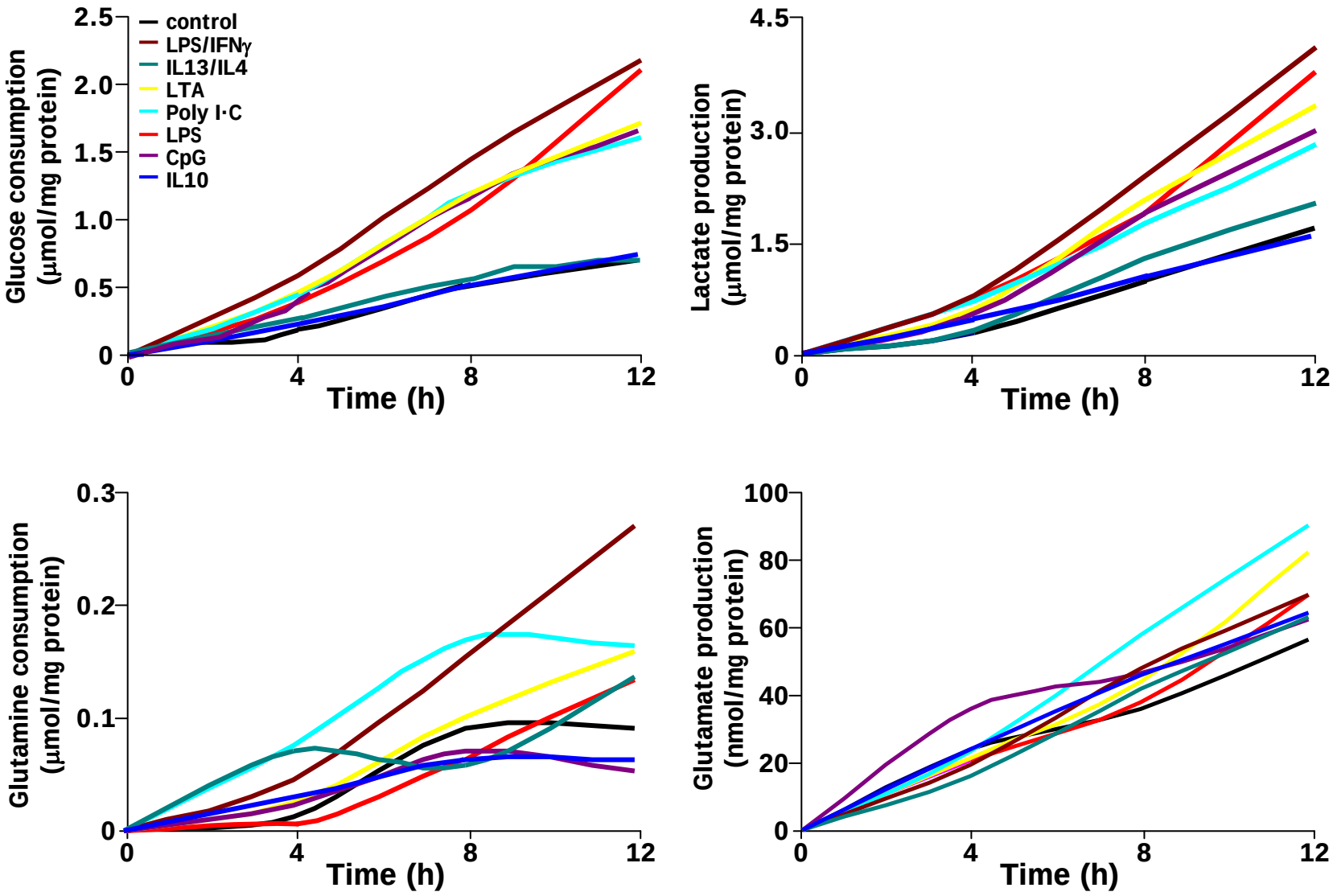

Fig. 2
Rod-Prados et al.

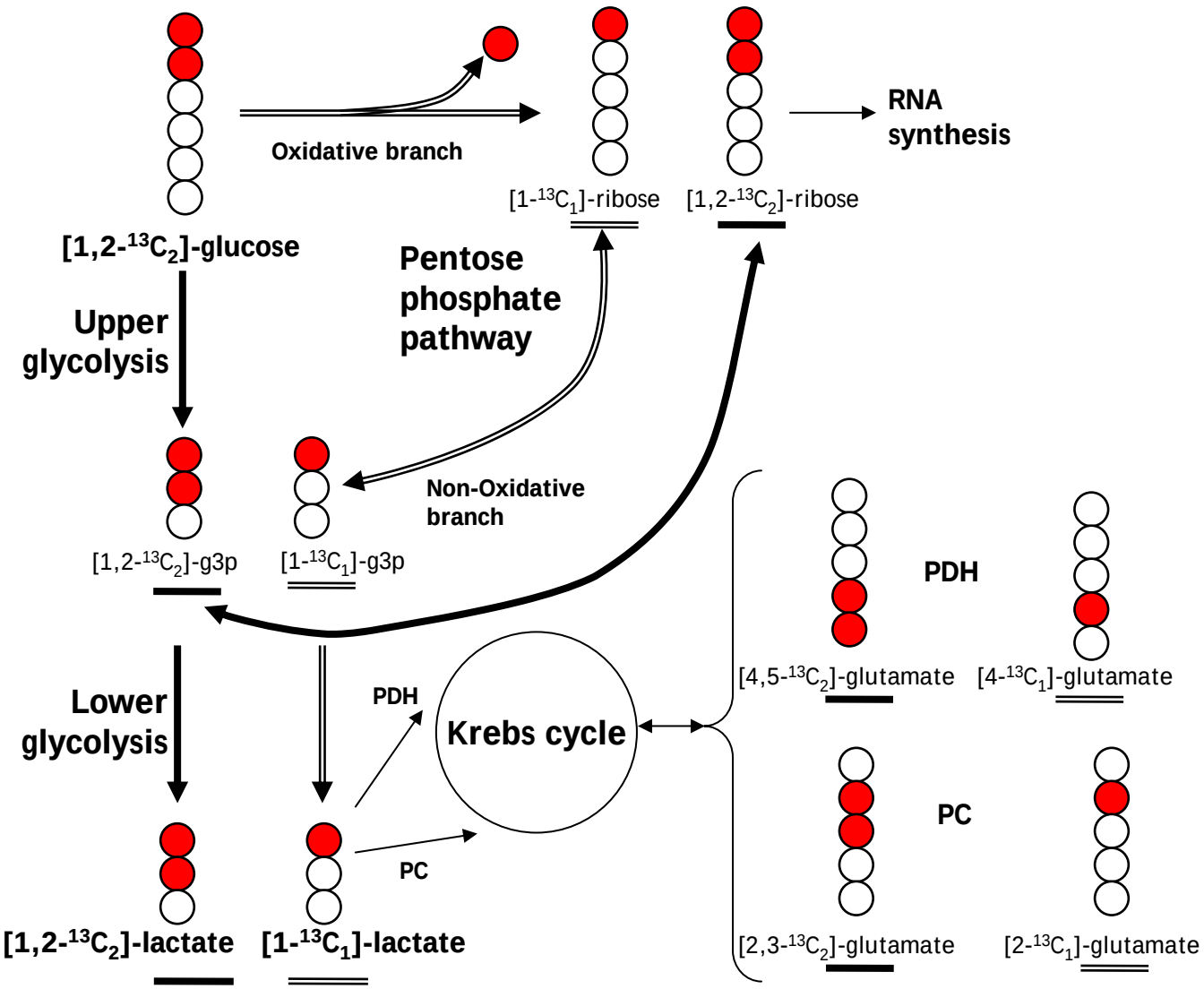

Fig. 3
Rod-Prados et al.

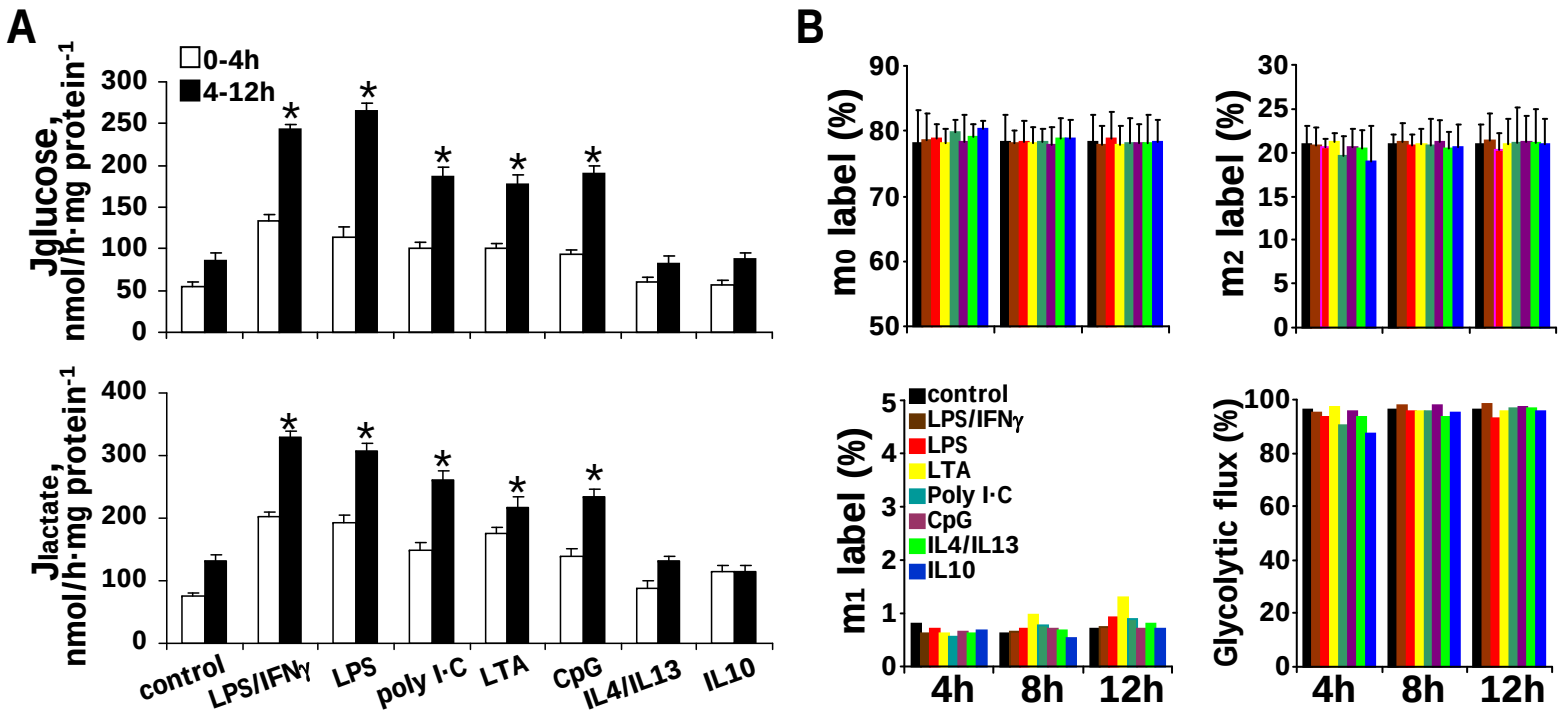

Fig. 4
Rod-Prados et al.

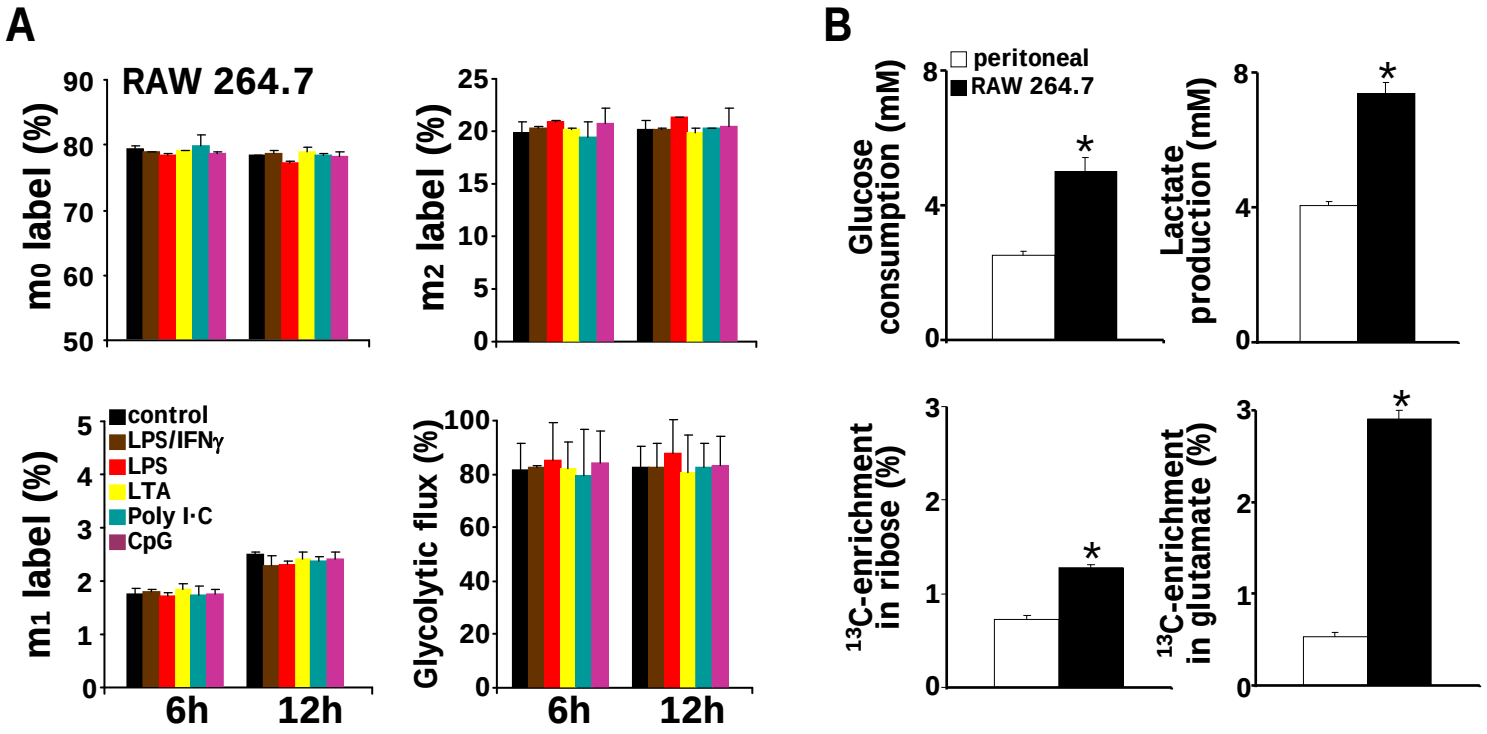

Fig. 5
Rod-Prados et al.

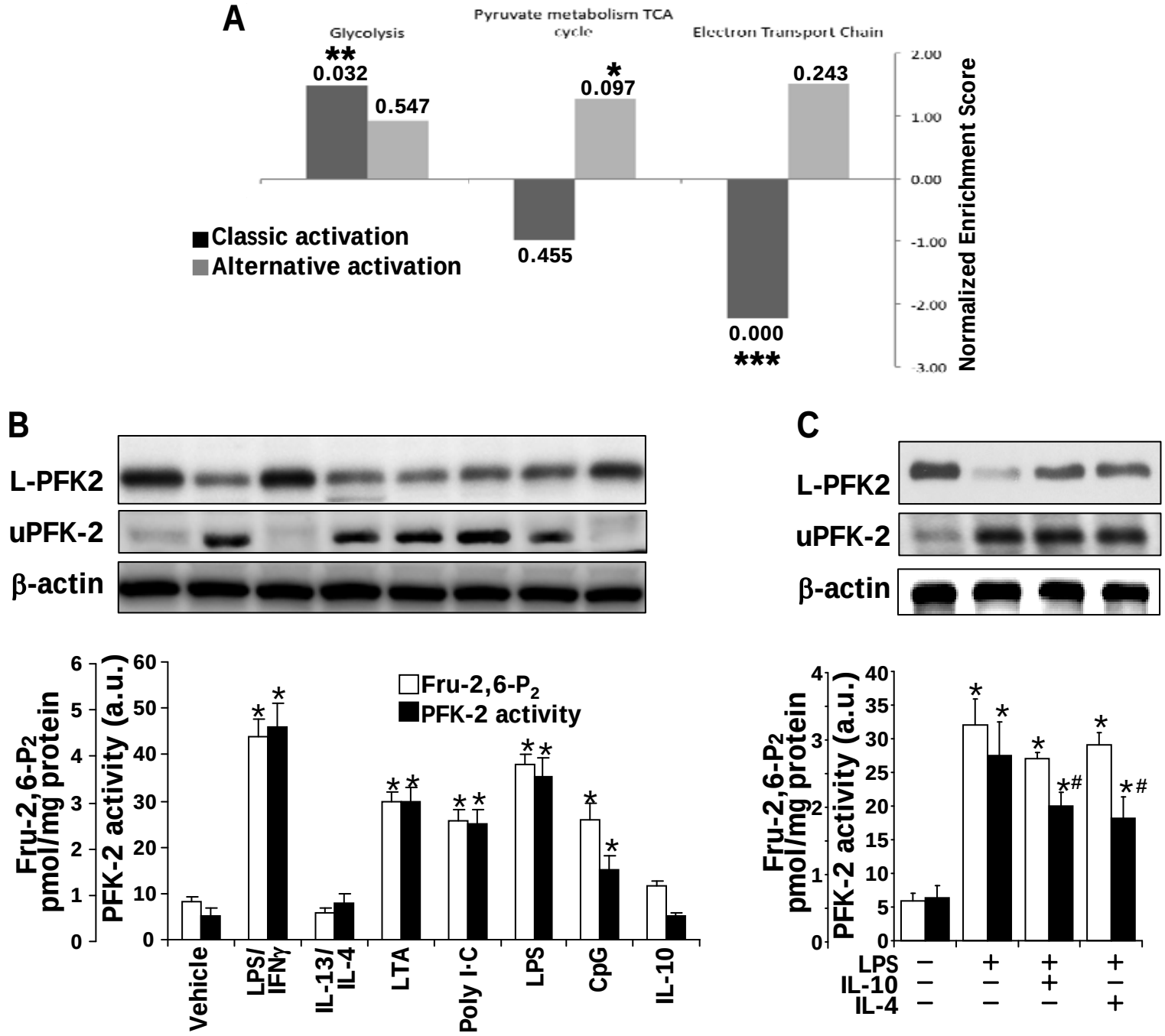

Fig. 6
Rod-Prados et al.

Fig. SUPPL 1
Rod-Prados et al.

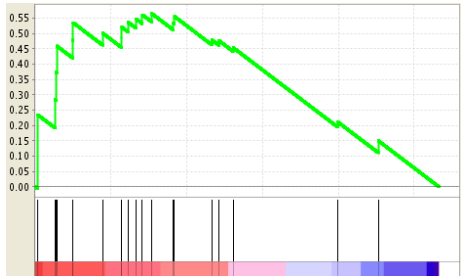

A. Glycolysis: Classic activation

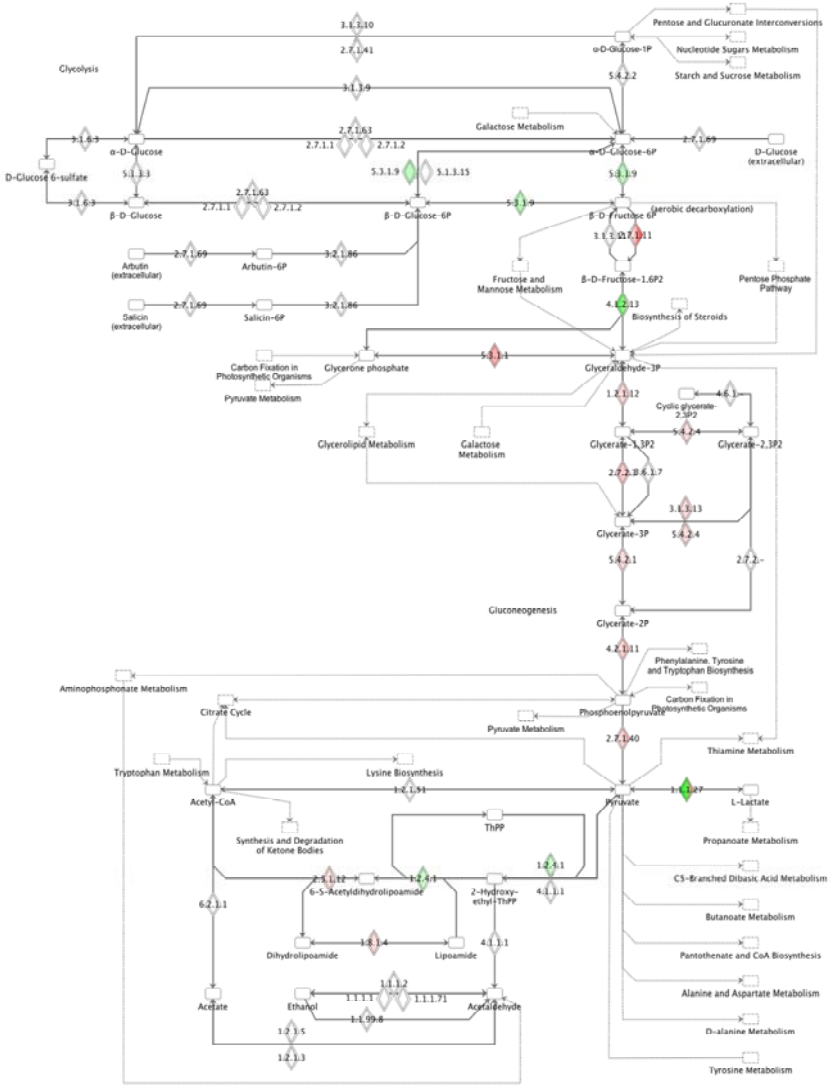

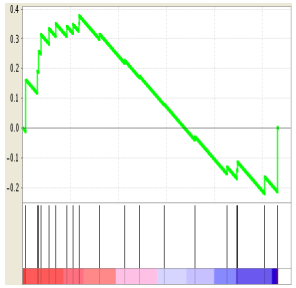

B. Glycolysis: Alternative activation

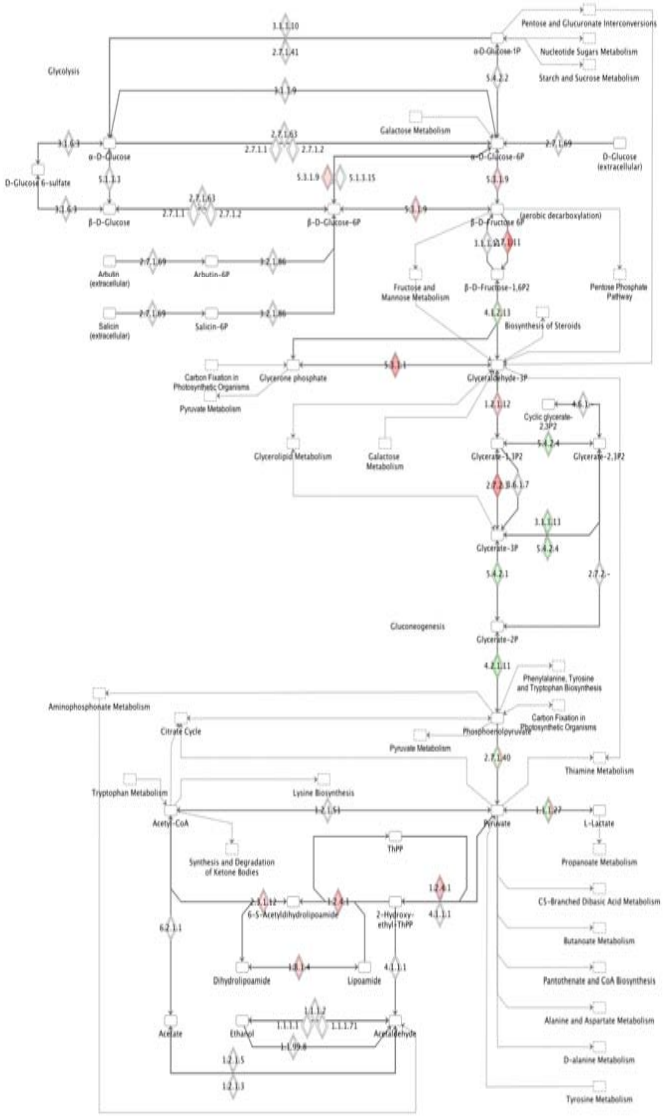

Fig. SUPPL 2
Rod-Prados et al.

A. Pyruvate metabolism and TCA: Classic activation

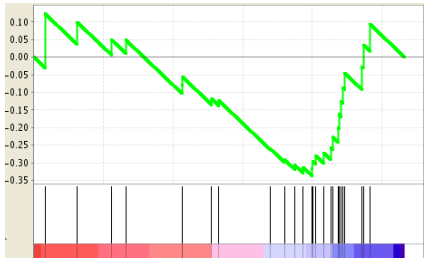

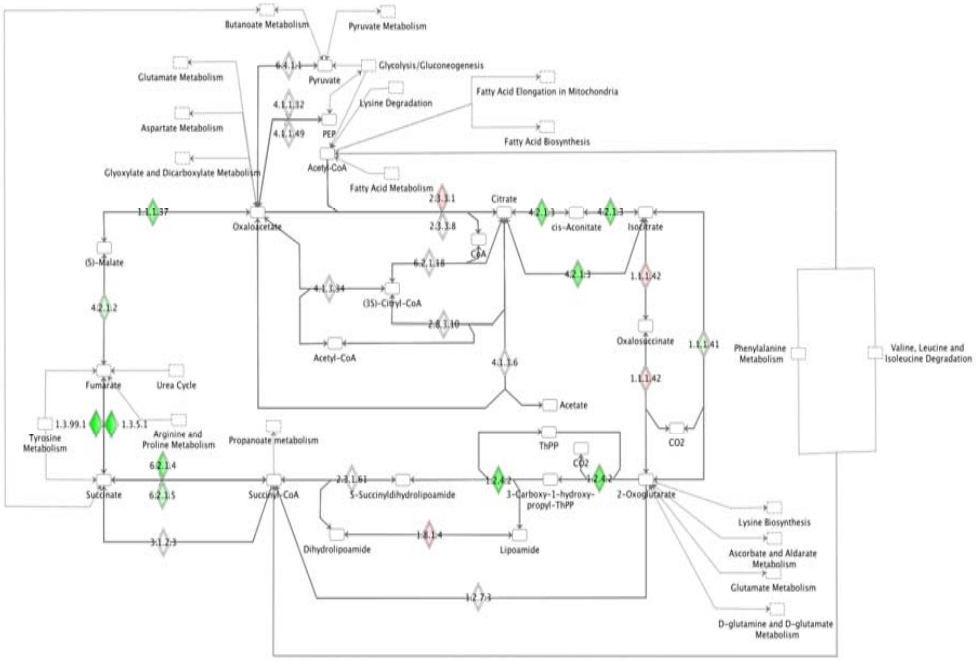

B. Pyruvate metabolism and TCA: Alternative activation

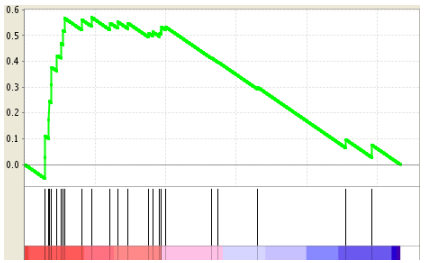

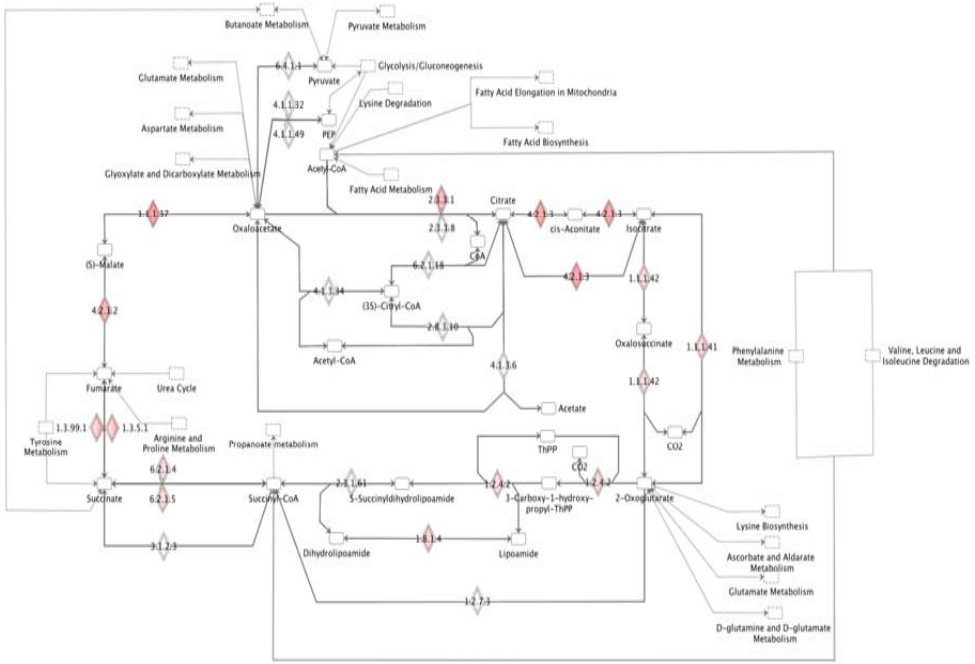

Fig. SUPPL 3
Rod-Prados et al.

A. Electron Chain Transport
Classic activation

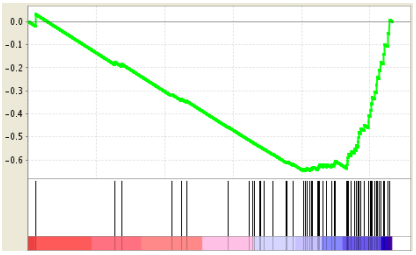

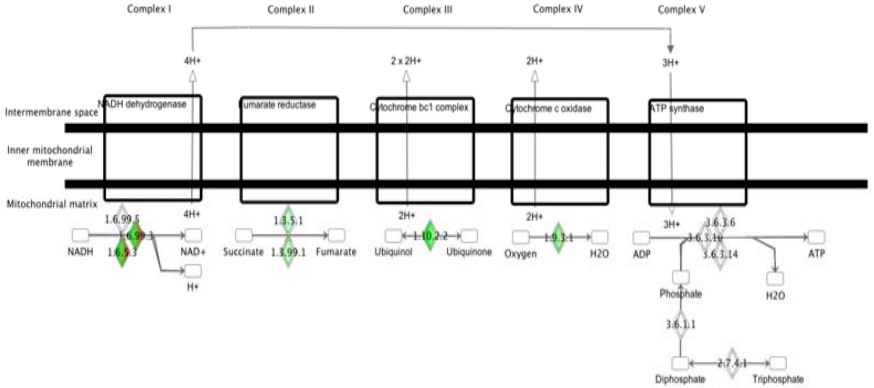

B. Electron Chain Transport
Alternative activation